Bulgarian Chemical Communications, Volume 50, Issue 3, (pp. 351 – 362) 2018

Synthesis, characterization and antioxidant measurements of selenium (IV) complexes with some amino acids - binuclear complexes

A. M. Naglah[1,2*], A. S. Al-Wasidi[3], N. M. Al-Jafshar[3], J. S. Al-Otifi[3], M. S. Refat[4, 5], R. F. Hassan[4,6] W. N. Hozzein[7,8]

[1] *Department of Pharmaceutical Chemistry, Drug Exploration & Development Chair (DEDC), College of Pharmacy, King Saud University, Riyadh 11451, Saudi Arabia*
[2]*Peptide Chemistry Department, Chemical Industries Research Division, National Research Centre, 12622-Dokki, Cairo, Egypt*
[3] *Department of Chemistry, College of Science, Princess Nourah Bint Abdulrahman University, Riyadh 11671, Saudi Arabia*
[4]*Chemistry Department, Faculty of Science, Taif University, P.O. Box 888, Al-Hawiah, Taif 21974, Saudi Arabia*
[5]*Department of Chemistry, Faculty of Science, Port Said, Port Said University, Egypt*
[6]*Chemistry Department, Faculty of Science, Helwan University, Cairo, Egypt*
[7]*Bioproducts Research Chair, Zoology Department, College of Science, King Saud University, Riyadh 11451, Saudi Arabia*
[8]*Botany and Microbiology Department, Faculty of Science, Beni-Suef University, Beni-Suef 62111, Egypt*

Received January 9, 2018; Accepted May 17, 2018

A series of selenium(IV) complexes of asparagine (*Asn*), proline (*Pro*), glutamine (*Gln*), methionine (*Met*) and cysteine (*Cys*) amino acids were prepared and well characterized based the (elemental analyses, molar conductance measurement), various spectral studies (IR, Raman, UV-Vis, ^{1}H-NMR and mass) and thermo gravimetric analyses (TG/DTG). The X-ray diffraction studies were carried out using PANalytical X-ray diffractometer, surface homogeneity of the respected samples was investigated using Quanta FEG 250 scanning electron microscope (SEM) and the chemical compositions of these samples have been studied using energy dispersive X-ray analyses. All the selenium (IV) complexes **(I-V)** are of $[Se^{+4}(AA^{-1})_2Cl_2]$ type, where AA = (*Asn*, *Pro*, *Gln*, *Met* and *Cys*) act as monobasic bidentate ligands in the synthesized complexes. Mass fragments of the [Se $(Cys)_2(Cl)_2$] (**V**) suggest monomeric statement. The speculated geometries of the 1:2 complexes were octahedral configuration with two chlorines and two bidentate ligands occupying the corners of the octahedral complexes. In selenium–*Asn*, *Pro*, *Gln*, and *Met* complexes both amino and carboxylate groups are involved in coordination with metal, but, *Cys* coordinates through its sulfhydryl and carboxylate groups. The free radical scavenging activity of newly synthesized selenium (IV) complexes was determined at the concentration of 10, 20 and 30 ppm by means of the interaction with free radical 1,1-diphenyl-2-picrylhydrazyl (DPPH) in stable form. All these complexes have a bullish antioxidant activity.

Keywords: Selenium; Amino acids; Raman; XRD; SEM; Nanorods; DPPH.

INTRODUCTION

Generally, amino acids containing two essential groups (amine and carboxylic acid) attached to the first α–carbon atom, are of particular importance in biochemical field. The chemical formula of α-amino acids is $H_2NCHRCOOH$ in most cases where, R is an organic substituent known as a side-chain [1, 2]. Amino acids are the main structural chemical constituents of proteins, which enter into the structure of all living organisms and are the most important factor in biochemical processes that support the preservation of human life [3, 4]. They are highly susceptible to being excellent catalysts and can be chelated with transition metals through their amino or carboxylic groups [5, 6]. Over the past few decades the complexation of transitional metal ions with amino acids has been studied [7, 8]. The amino acid reactions were found to be responsible for the enzymatic activity and stability of protein structures [9, 10]. The complexity of mineral amino acids is an important area of research where they can be used as simulated systems to identify the interaction of mineral protein in biological systems.

Selenium is one of the rarer elements present in low and fundamental concentrations in the human body and is of great importance in nutrition and medicine [11]. Selenium nanoparticles have some unique optical, mechanical, electrical, biological and chemical properties as compared to other chemicals. For example, selenium nanoparticles have been reported to have high biological activity and low toxicity [12], and nanowires of selenium with trigonal geometry have new optical photoconductivity [13]. Thus, selenium

* To whom all correspondence should be sent:
E-mail: amnaglah@gmail.com

nanoparticles attracted considerable interest of researchers and different synthesis methods were exploited [14-17].

Amino acid coordination chemistry is an integral feature of inorganic and bioinorganic chemistry [18-20], with many applications in medicinal design and materials science [21, 22]. Selenium amino acid complexes attract attention of chemists because of their different kinds of applications. In selenium (IV) amino acid complexes syntheses, the amino acid is first reacted with a selenium (IV) ion and gives stable octahedral selenium (IV) complexes. In this paper an overview on structures and coordination chemistry of selenium (IV) amino acid complexes is given. This article describes the synthesis of selenium nanoparticles by *in situ* amino acid chelation. This study presents preliminary results of synthesized bis-chelated complexes of the used five amino acids, shown in Fig. 1.

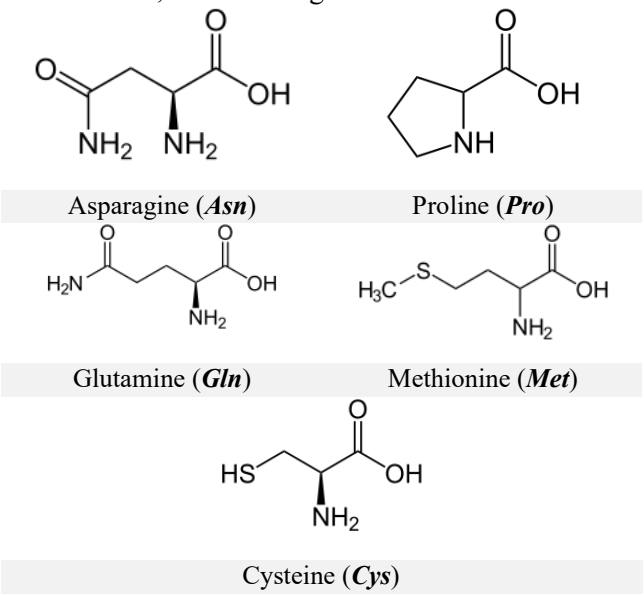

Fig. 1: Chemical structures of the used five amino acids

MATERIALS AND METHODS

Chemicals and reagents

The amino acids (L-configuration) asparagine (*Asn*), proline (*Pro*), glutamine (*Gln*), methionine (*Met*) and cysteine (*Cys*) were purchased from Sigma-Aldrich Chemical Company, all organic solvents and reagents were used in pure form. $SeCl_4$ was received from Aldrich Company.

Synthesis of selenium (IV) amino acid complexes

The collected compounds were prepared using the same chemical procedures, as follows: adding 25 mL of amino acids in ethanol (4 mmol) to the same volume of selenium (IV) tetrachloride also in ethanol (2 mmol). The solutions were refluxed for 2 h and the resultant brown to black-brown solution was reduced to *ca*. 1/2 of its volume. The solids produced by filtration were collected and washed with petroleum ether (60-80°C) and dried in a vacuum medium over anhydrous $CaCl_2$.

Instruments

– Elemental analysis (%C, %H and %N) percentage was performed using Perkin Elmer CHN 2400.

– Molar conductivity (10^{-3} mol/cm^3) with dimethylsulfoxide (DMSO) solvent was determined using Jenway 4010 conductivity meter.

– Electronic spectra were scanned using UV-3101 PC Shimadzu spectrophotometer.

– FT-IR spectra were scanned on a Bruker FT-IR spectrophotometer.

– Raman laser spectra were collected on a Bruker FT-Raman spectrophotometer equipped with a 50 mW.

– ^{1}H-NMR spectra were recorded using a Varian Gemini 200 MHz spectrometer.

– Mass spectra were scanned using AEI MS 30 mass spectrometer with 70 eV.

– Thermal study TG/DTG–50H was carried out on a Shimadzu thermogravimetric analyzer under nitrogen atmosphere.

– Scanning electron microscopy (SEM) was performed on Quanta FEG 250 equipment.

– X-ray powder diffraction was measured on X'Pert PRO PANanalytical with target Cu with secondary monochromator.

DPPH and Hydroxyl Radical Scavenging assays

The 2, 2-diphenyl-1-picrylhydrazyl (DPPH) assay was performed as described in [23]. Free radical damage imposed on the substrate, deoxyribose, was measured using the thiobarbituric acid test [24, 25]. The inhibition (I) percentage of deoxyribose degradation was experimentally calculated using the following relationship:

$$I\ (\%) = 100 \times (A_0\text{-}A_1/A_0)$$

where A_0 is the absorbance of the control sample and A_1 is the absorbance of the tested sample. Statistical analysis: each of the measurements described was conducted in at least three identical trials and the results were reported as mean and standard deviation, significantly different calculated level at $p \leq 0.05$.

RESULTS AND DISCUSSION

Microanalysis results

Analytical results for the synthesized selenium (IV) amino acid complexes are listed in Table 1.

Table 1: Elemental analysis and physical data of $[Se^{+4}(AA^{-1})_2Cl_2]$ complexes

Complex/ Empirical formula	M. wt. g/mole	% C (calcd.)/found	% H (calcd.)/found	% N (calcd.)/found	Mp/°C	*Color*	Λm ($\Omega^{-1}cm^2\,mol^{-1}$)
$[Se(Asn)_2(Cl)_2]$ $C_8H_{14}Cl_2N_4O_6Se$, **I**	412.09	(23.32) 23.21	(3.42) 3.39	(13.60) 13.54	179	Brown	27
$[Se(Pro)_2(Cl)_2]$ $C_{10}H_{16}Cl_2N_2O_4Se$, **II**	378.11	(31.77) 31.65	(4.27) 4.23	(7.41) 7.40	185	Brown	25
$[Se(Gln)_2(Cl)_2]$ $C_{10}H_{18}Cl_2N_4O_6Se$, **III**	440.14	(27.29) 27.18	(4.12) 4.10	(12.73) 12.70	210	Red brown	43
$[Se(Met)_2(Cl)_2]$ $C_{10}H_{20}Cl_2N_2O_4S_2Se$, **IV**	446.27	(26.91) 26.88	(4.52) 4.50	(6.28) 6.26	201	Red brown	32
$[Se(Cys)_2(Cl)_2]$ $C_6H_{12}Cl_2N_2O_4S_2Se$, **V**	390.17	(18.47) 18.42	(3.10) 3.07	(7.18) 7.15	245	Black brown	38

These support the formation of binuclear complexes with chemical composition of 1:2 selenium to amino acid stoichiometry. All complexes are colored, and soluble in DMF and DMSO. The elemental analysis in Table 1 matched well with 1:2 (Se: amino acid) ratio. For selenium complexes, the molar conductivities are in the range of 25-43 ohm^{-1} cm^2 mol^{-1}. These values deduced that 1:2 complexes are non-electrolytes soluble in DMSO [26, 27]. These results are regarded to be low due to the existence of the two chlorine atoms inside the coordination sphere. These complexes have a melting point within the 179-245 °C range, with yield of 80-88%. The presence of Cl^- ions was checked using $AgNO_3$ reagent.

Electronic spectra

The shift of *n*-π* characteristic band in the UV-Vis spectra, attributed to the C=O bond (272 nm for *Asn*-Se, 272 nm for *Pro*-Se, 276 nm for *Gln*-Se, 294 nm for *Met*-Se and 264 nm for *Cys*-Se) is due to the involving of the non –bonding electron pairs of the oxygen in the metal-ligand bond formation, Fig. 2. The formation of amino acids SeNPs was confirmed with the help of UV–Vis spectra investigation according to the change in color from colorless (selenium(IV) chloride) to three degrees of brown color (SeNPs), having absorption maximum λ_{max} at 300–400 nm [28].

Infrared spectra

FT-IR spectra of the five investigated complexes are illustrated in Figs. 3a-e. These spectra display very similar spectral bands, so the coordination behavior in all selenium (IV) complexes **I-V** is similar. The proposed spectral assignments are presented in Table 2.

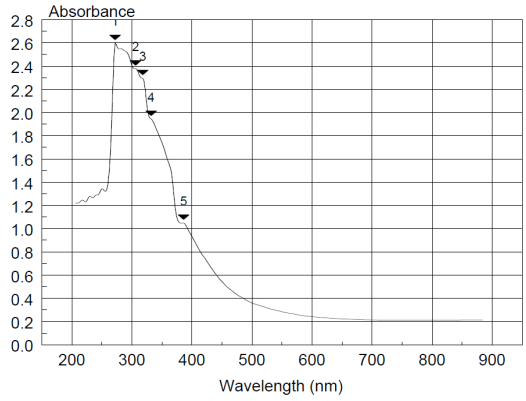

a

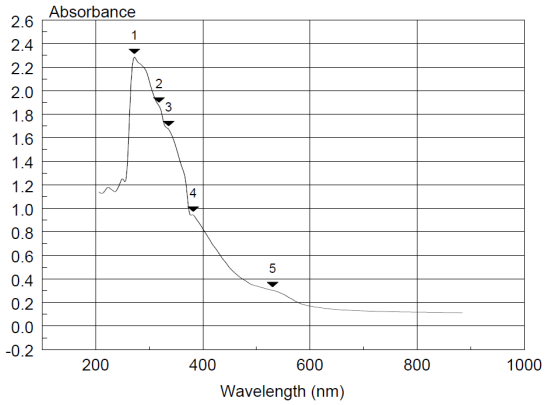

b

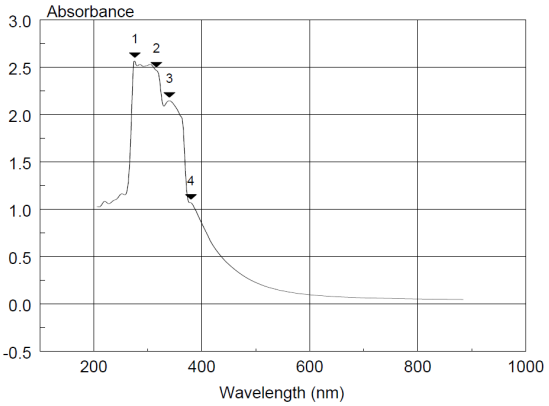

c

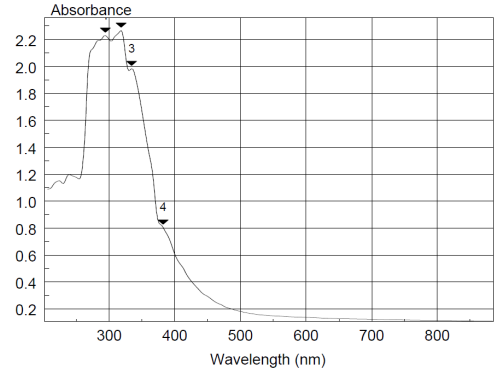

d

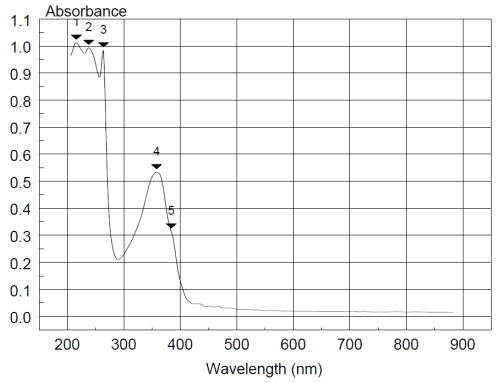

e

Fig. 2. UV-Vis spectra of $[Se(AA)_2Cl_2]$ complexes: a- *Asn*, b- *Pro*, c- *Gln*, d- *Met,* e- *Cys*.

The assignments were discussed on the basis of literature [29-31] and with the help of some interesting references [32, 33]. The characteristic bands were referred to CH, CH_2 and CH_3 deformational modes, and other skeletal vibrations between 2980-2900 cm^{-1} with similar energies in all spectra.

– The O–H stretching modes are overlapped with the $–NH_2$ stretchings around 3000-3200 cm^{-1}.

– The free amino acids exist as zwitterions in the solid state, thus, there are two stretching vibrations for the COO− moiety present in these systems, namely ν_s(COO−) and ν_{as}(COO−).

– The ν_s(COO−) usually has a medium intensity in the IR spectrum, whereas the ν_{as}(COO−) has a strong broad band.

– After coordination, one should expect a lowering of the frequency of one of these bands, due to the generation of a Se–O bond and the energy increase of the other, because the C–O double bond is partially reconstructed, as it can be seen from the data presented in Table 2.

– The absence of the characteristic $\nu(NH_3^+)$ and $\delta(NH_3^+)$ bands and the shift in the position of the carboxylate stretching vibrations in the free ligand, clearly confirm its existence in the non zwitterionic form.

In the spectrum of selenium (IV)-*Cys* complex, the infrared frequencies at 1622 and 1407 cm^{-1} were assigned to antisymmetric and symmetric COO^- frequencies, respectively. In free *Cys* the SH frequency appears at 2548 cm^{-1} but the infrared spectrum of Se(IV)–*Cys* complex shows no SH absorption frequency. The absence of SH frequency in the spectrum of the complex is an evidence of the involvement of S group in complexation with metal. The NH_2 frequencies are found to be at 3027, 1487 and 1125 cm^{-1}. Antisymmetric and symmetric COO^- frequencies in Se-*Asn*, Se-*Pro*, Se-*Gln* and Se-*Met* complexes are at (1667 and 1403) cm^{-1}, (1621 and 1403) cm^{-1}, (1593 and 1402) cm^{-1}, and (1617 and 1409) cm^{-1}, respectively. There are no NH_2 bending frequencies in the spectra of these complexes as expected from the symmetry consideration. The complexes exhibit two new frequencies at 600-500 and 500-400 cm^{-1}, respectively, due to Se-O and Se-N stretching [33]. The Se-*Gln* complex has medium string band at 1682 cm^{-1} attributed to stretching vibration of the carbonyl of the amido group. From IR data, the energy difference between both $\nu_{as}(COO^-)$ and $\nu_s(COO^-)$ vibrations (Δ = 191-264 cm^{-1}) clearly supports the participation of carboxylate group in monodentate binding [34].

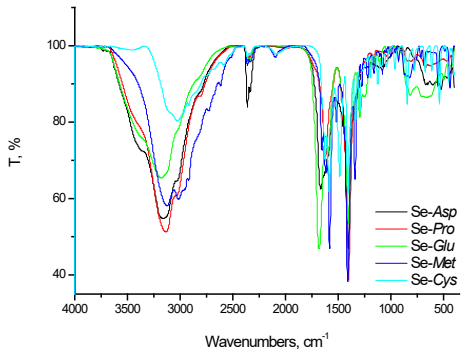

Fig. 3. Infrared spectra of $[Se\ (AA)_2Cl_2]$ complexes (AA= *Asn*, *Pro*, *Gln*, *Met* and *Cys*).

The infrared spectra of the bi-chelated Se (IV) complexes of the amino acids *Asn*, *Pro*, *Gln*, *Met* and *Cys* were recorded and analyzed in relation to their structure, Fig. 4.

Proton Magnetic Resonance Spectra

The chemical shifts of Se-*Cys* (**V**) complex are shown in Fig. 6. The spectrum of complex **V** possesses two characteristic signals. The sharp signal due to the –CH and –a CH2 proton is observed around 3.31 ppm. The singlet broad signal of the $–NH_2$ protons is located at 7.01 ppm. The resonance due to the proton of the –OH and –SH groups (11-12 ppm) of the *Cys* chelate disappears in the selenium (IV) complex (**V**) indicating that coordination has taken place through the

deprotonation of –OH and binding of S atom of –SH group. Finally, the presence of a singlet broad band at 7.01 ppm is due to the faraway of nitrogen atom of $–NH_2$ from complexation, Fig. 4.

Table 2. IR frequencies (cm^{-1}) of $[Se(AA)_2Cl_2]$ complexes

Compound	ν(O-H) ν(N-H)	ν(COO^-)		δ(NH_2)	ν(M-O)	ν(M-N)
		Asym	Sym			
I	3163	1667	1403	--	524	466
II	3136	1621	1403	--	520	470
III	3180	1593	1402	--	497	428
IV	3124	1617	1409	--	523	439
V	3027	1622	1407	1487	540	455

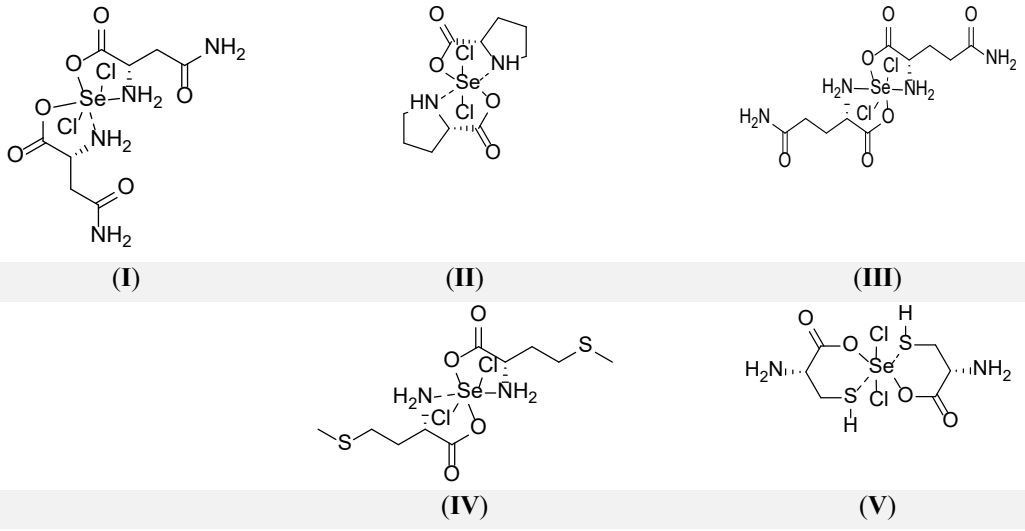

Fig. 4. Speculated structures of $[Se(AA)_2Cl_2]$ complexes (AA= *Asp*, *Pro*, *Glu*, *Met* and *Cys*).

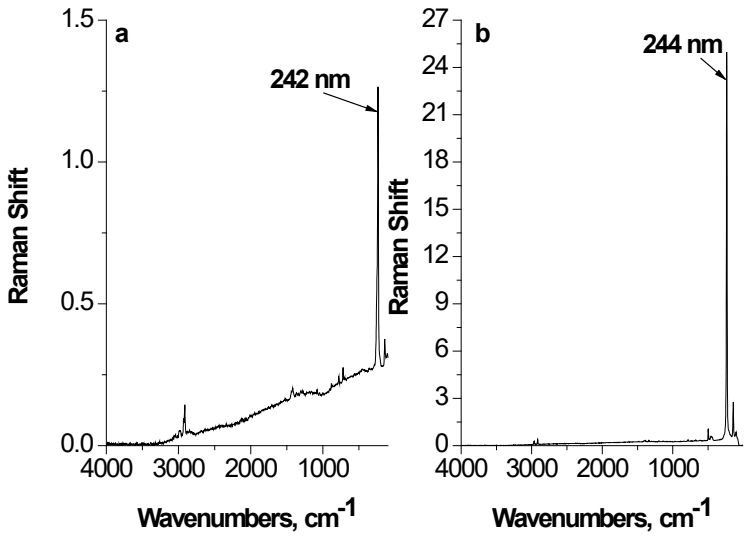

Fig. 5. Raman laser spectrum of a- Se-*Met* and b- Se-*Cys* complexes

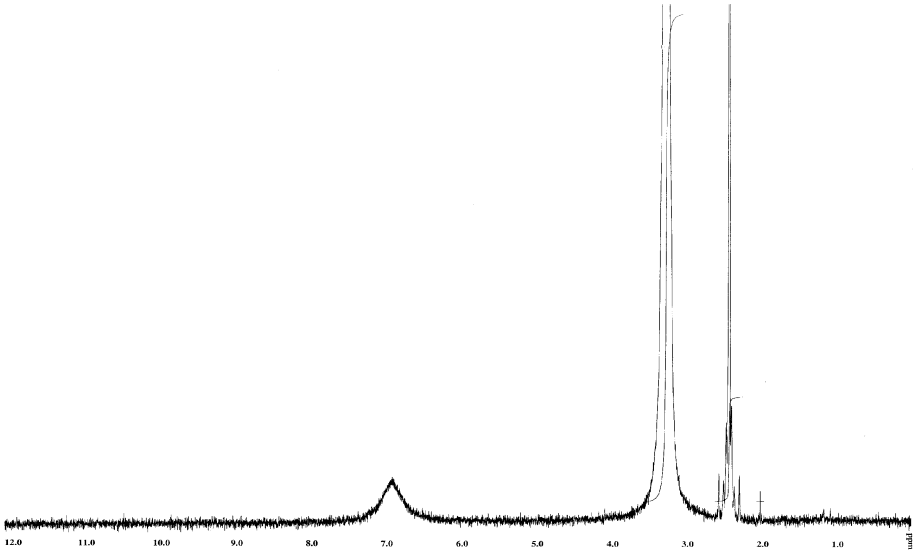

Fig. 6. [1]H-NMR spectrum of the Se-*Cys* complex.

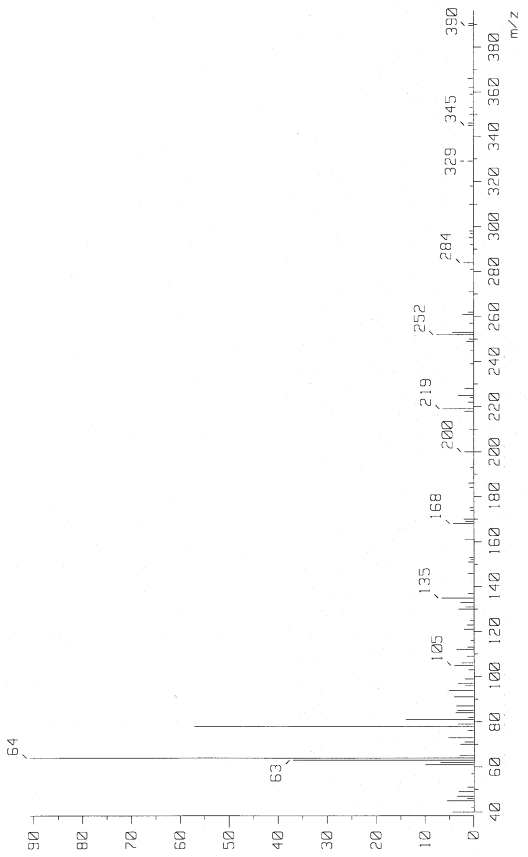

Fig. 7. Mass spectrum of Se-*Cys* complex.

Mass Spectra

Chemical shifts of the Se-Cys (V) complex: The mass spectral data of the [Se(*Cys*)$_2$(Cl)$_2$] complex are presented in Fig. 7. The mass spectrum of Se-*Cys* complex showed a molecular ion peak that is in a good agreement with the expected value. The mass spectrum of Se-*Cys* shows a peak at 390 m/z, which was assigned as a [M] peak. The *Cys* molecule was thought to produce ions at m/z 345, 329, 284,252, 219,200, 168, 135, 105, 64, and 63, respectively. The m/z 78 ion, which is a Se-*Cys* (**V**) complex, is containing one selenium atom.

XRD Spectra

The X-ray diffraction patterns of the [Se(*Cys*)$_2$(Cl)$_2$] complex with selenium nanoparticles are shown in Fig. 8. The diffraction peaks present at 2θ (degrees) of 23.42°, 29.57°, 42.05°, 43.75°, 45.47°, 51.43°, 55.70°, 61.46°, 65.09° and 71.59° correspond to (100), (101), (110), (102), (111), (201), (112), (202), (210) and (113) planes of selenium, respectively. The diffraction peaks within the 2θ region due to hexagonal crystal structure of selenium are in agreement with the standard data (JCPDS card No. 01-071-4647), as shown in Fig. 9. The particle size of selenium was estimated using Scherrer's eq. [36]

$$D = \frac{0.89\lambda}{\beta \cos\theta} \qquad 1$$

where D = grain size, K = constant equal to 0.94, λ = wavelength of the X-ray radiation, β = full width at half maximum and θ = diffraction angle. The particle size of selenium nanoparticles is found to be ~ 10 nm. The diffraction pattern due to (100), (101), (110), (102), (111) and (201) directions of hexagonal phase of selenium is shown in Fig. 9. The d-spacing values for the diffraction pattern match well with the hexagonal selenium.

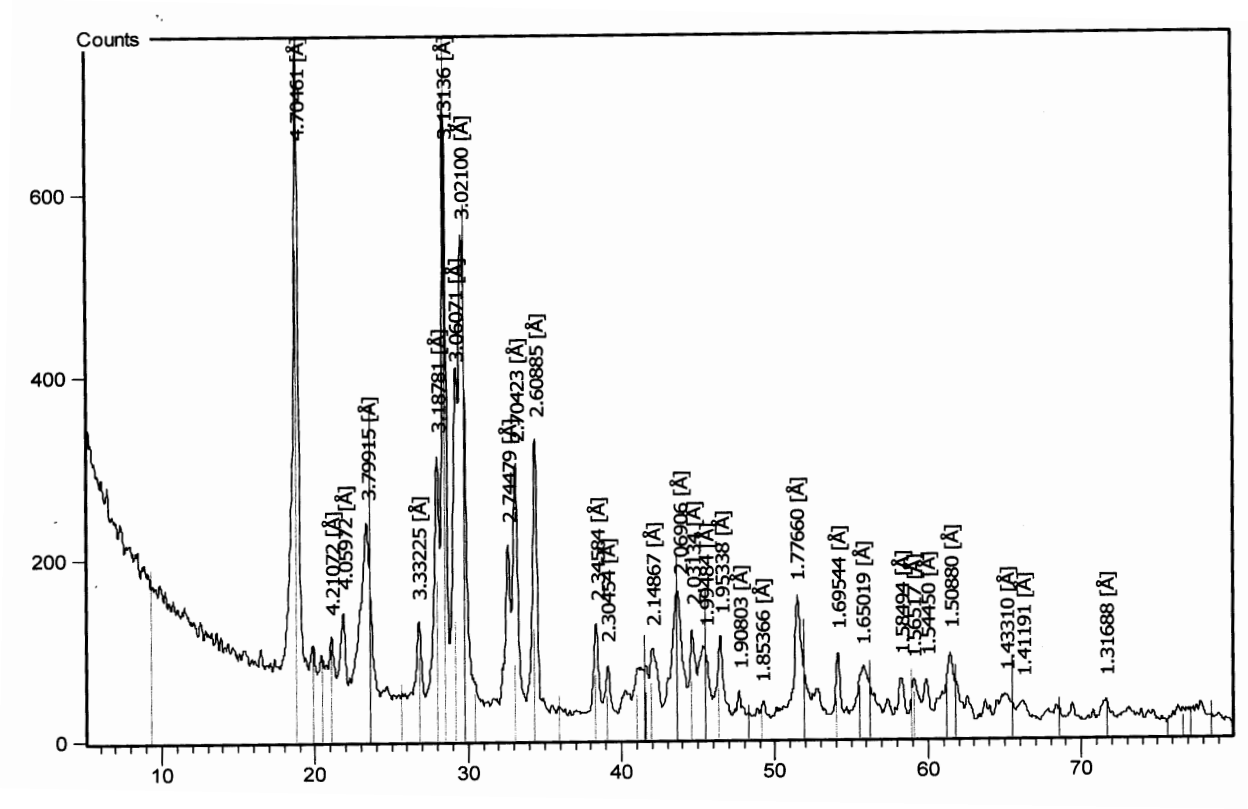

Fig. 8. XRD spectrum of Se-*Cys* complex.

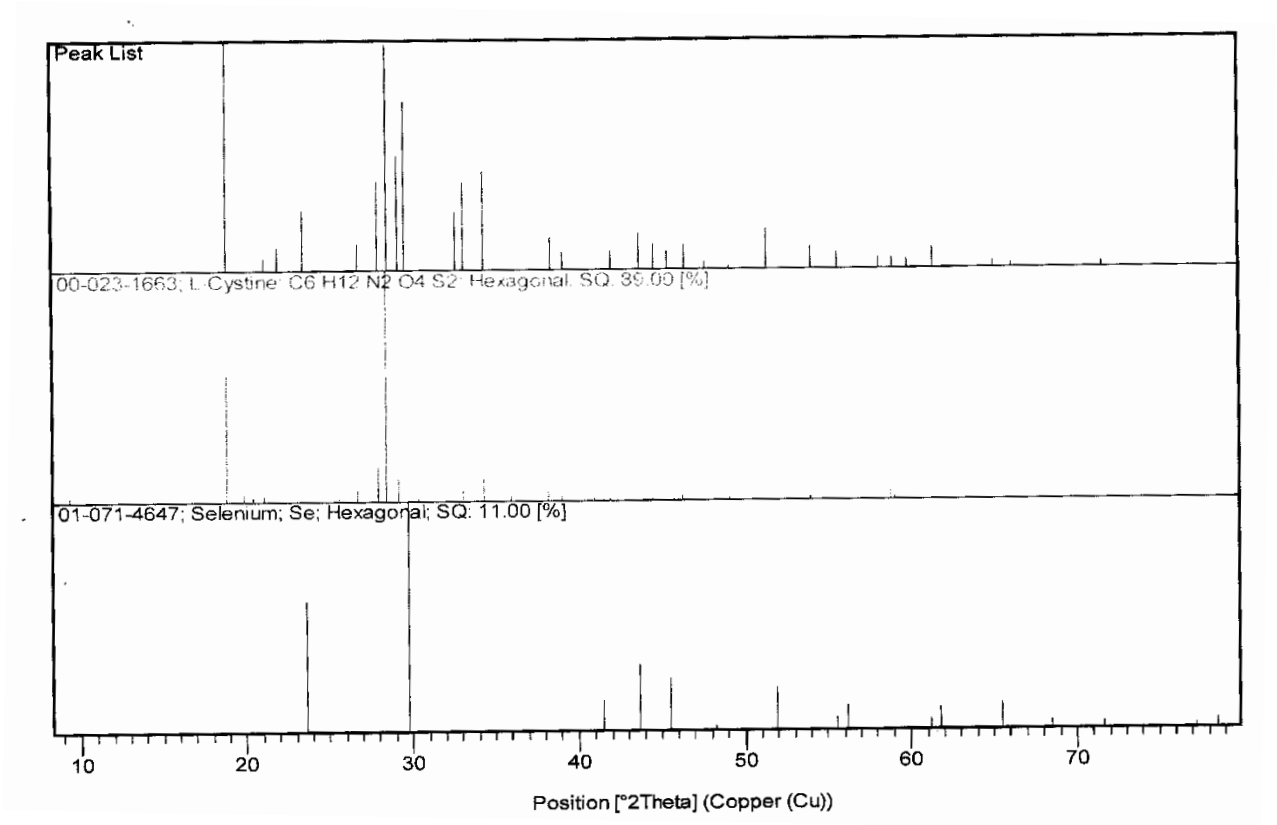

Fig. 9. Standard XRD spectrum of *Cys* and Se-*Cys* complex with selenium hexagonal structure.

SEM, TEM and EDX Spectra

The scanning electron microscope (SEM) image of the [Se(*Cys*)$_2$(Cl)$_2$] complex with selenium nanorods and hexagonal structure is illustrated in Fig. 10. The SEM image reveals that the selenium nanorods are of uniform size with a mean diameter of ~ 10 nm. It can be seen that nanorods are of several micrometers in length with diameter ranging from 10 μm. Energy dispersive X-ray analysis (EDX) was used to identify and determine the chemical composition of the Se-*Cys* complex. EDX pattern of the Se-*Cys* complex is shown in Fig. 11. Weak signals concerning O atoms have been recorded along with the strong peak due to Se atom. EDX analysis indicates the presence of O, S, C, and Cl with very low intensity, so this analysis supported the purity of the selenium particles.

The transmission electron microscopy images were performed using JEOL 100s microscope. Fig. 12 shows the transmission electron microscope (TEM) image of Se-*Cys* complex selenium nanorods. The image shows that the nanorods are with an average diameter of ~ 10 nm.

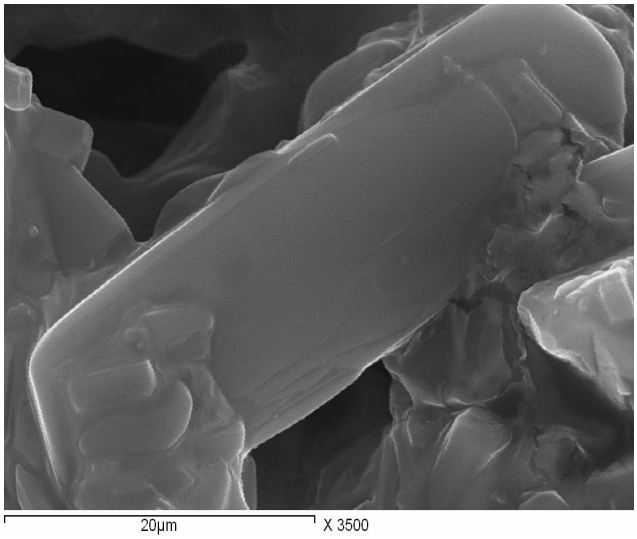

Fig. 10: SEM image of Se-*Cys* complex.

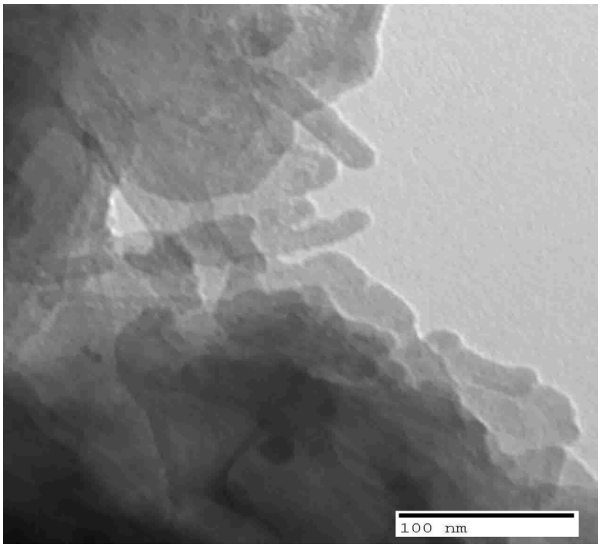

Fig. 12. TEM image of Se-*Cys* complex

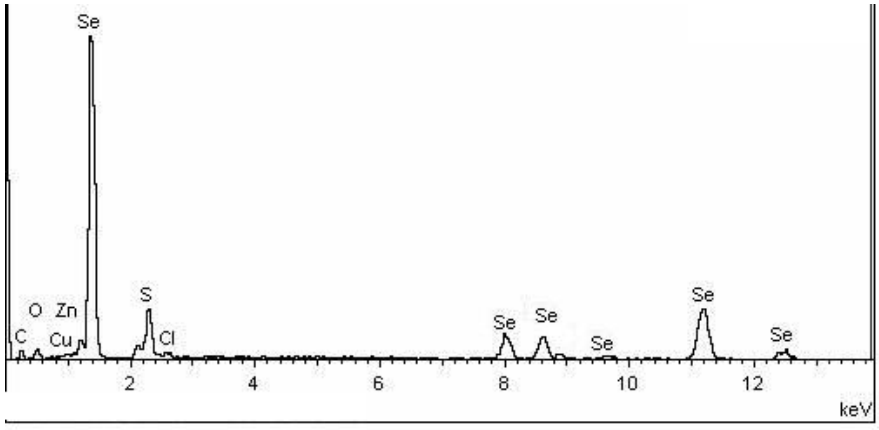

Fig. 11. EDX spectrum of Se-*Cys* complex.

Thermal analysis

Thermal stability of [Se(AA)$_2$Cl$_2$] complexes (AA= *Asn*, *Pro*, *Gln*, *Met* and *Cys*) complexes was checked based on thermo gravimetric and its differential analyses started from room temperature till 800 ºC under N_2 atmosphere. The TG curves were redrawn as mg mass loss *versus* temperature. The thermal decomposition curves (TG) are given in Fig. 13.

Asn-Se complex: Thermal decomposition of *Asn*-Se complex (**I**) occurs in four steps. The 1st degradation step takes place in the temperature range of 179-222 ºC at DTG$_{max}$ = 196 ºC (endo) and it correspond to a mass loss of 15.043%. The 2nd step occur within the temperature range of 296-367 ºC at DTG$_{max}$ = 317 ºC (endo) which was assigned to the decomposition of *Asn* molecule with a weight loss of 52.949%. The 3rd step occurs within the

temperature range of 433-475 °C at DTG_{max} = 452 °C which is due to loss of organic moiety with a weight loss of 8.835%. The last decomposition step takes place within the temperature range of 573-663 °C with mass loss of 21.464%. The residual carbon atoms (1.709%) in the final product remain stable till 800 °C.

Pro-Se complex: The thermal decomposition of *Pro*-Se complex (**II**) occurs in three steps. The first degradation step takes place in the temperature range of 121-167 °C at DTG_{max} = 136 °C (endo) and it corresponds to the loss of one chlorine atom with mass loss of 7.697%. The second step occurs within the temperature range of 275-383 °C at DTG_{max} = 325 °C (endo) which was assigned to the decomposition of two *Pro* and one chlorine molecule with weight loss of 75.077%. The third step occurs within the temperature range of 527-625 °C at DTG_{max} = 563 °C (endo) which was assigned to the loss of organic moiety with a weight loss of 12.420%. The few carbon atoms in the final product remain stable till 800 °C with mass loss of 4.806%.

Gln-Se complex: The thermal decomposition of *Gln*-Se complex (**III**) occurs in four successive steps. The first degradation step takes place in the temperature range of 46-55 °C at DTG_{max} = 44 °C and it corresponds to the loss of water molecules with a weight loss of 2.183%. The second step occurs within the temperature range of 156-202 °C at DTG_{max} = 172 °C (endo) which was assigned to the loss of one of the chlorine molecules beside the amino terminal groups with a weight loss of 10.069%. The third step occurs within the temperature range of 284-381 °C at DTG_{max} = 328 °C (endo) which was assigned to the loss of organic moiety of *Gln* chelate with a weight loss of 54.740%. The fourth step occurs within the temperature range of 432-800 °C at DTG_{max} = 500 °C which was assigned to the loss of organic moiety with a weight loss of 8.102%. The few carbon atoms with mass (24.906%) in the final product remain stable till 800 °C.

Met-Se complex: The thermal decomposition of *Met*-Se complex (**IV**) occurs in three steps. The first degradation step takes place in the temperature range of 128-146 °C at DTG_{max} = 134 °C (endo) and it corresponds to the loss of chlorine atoms with a weight loss of 11.363%. The second step occurs within the temperature range of 257-303 °C at DTG_{max} = 277 °C (endo) that was assigned to the loss of organic moiety with a weight loss of 56.139%. The third step occurs within the temperature range of 494-535 °C at DTG_{max} = 511 °C that was assigned to the loss of organic moiety with a weight loss of 10.147%. The residual carbon with a mass of 2 2.351% in the final product remains stable till 800 °C.

Cys-Se complex: The thermal decomposition of *Cys*-Se complex (**V**) occurs in three successive steps. The first degradation step takes place in the temperature range of 265-305 °C at DTG_{max} = 284 °C and it corresponds to the loss of two chlorine atoms and two molecules of *Cys* with weight loss of 70.559%. The second step occurs within the temperature range of 381-436 °C at DTG_{max} = 397 °C which was assigned to the loss of organic moiety with a weight loss of 12.665%. The third step occurs within the temperature range of 448-558 °C at DTG_{max} = 509 °C (endo) which was assigned to the loss of organic moiety with a weight loss of 11.700%. The residual few carbon atoms with m(VO_2 + C) in the final product remain stable till 800 °C as a final residue.

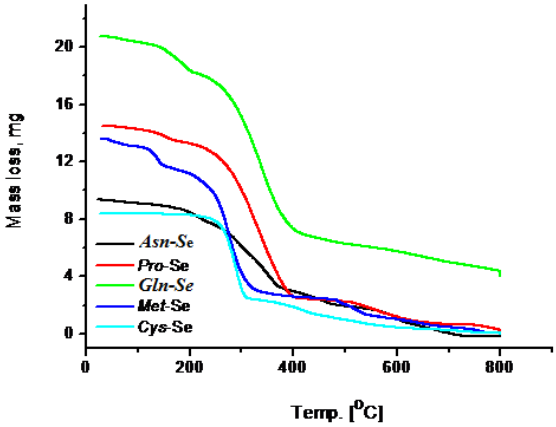

Fig. 13. TG curves of $[Se(AA)_2Cl_2]$ complexes (AA= *Asn*, *Pro*, *Gln*, *Met* and *Cys*).

Antioxidant activity

Bioavailability of selenium from dietary supplements is strongly dependent on its chemical form. Seleno amino acids which possess organically bound selenium are considered to be better absorbed and less toxic than inorganic selenium compounds [37]. Many chemical materials have been evaluated for antioxidant activities using *in vivo* and *in vitro* models and the selenium compounds trial is one of the most successful. The aim of this work was to examine the antioxidant activities of five selenium amino acid complexes. DPPH and hydroxyl radical scavenging methods were applied to *in vitro* models. Resulted data indicated that the radical scavenging activities of the tested compounds depend on the chemical form of selenium. Radical scavenging activity effects of selenium complexes

I-V against DPPH and hydroxyl radicals are shown in Figs. 14 and 15. All concentrations (10, 20 and 30 ppm) of the tested complexes showed significant to moderate radical scavenging activity compared to standard BHA material (70.4, 85.1 and 94.3%), respectively. As shown in Figs. 14 and 15, the radical scavenging activity of all tested compounds gradually increases through all concentrations (10, 20 and 30 ppm) compared with butylated hydroxyanisole (BHA) as positive control.

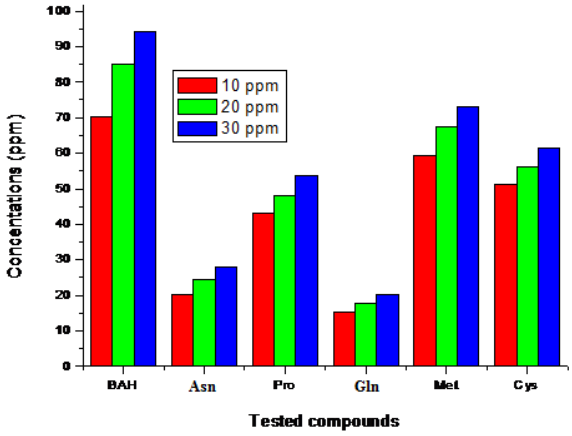

Fig. 14. Diagrams of radical scavenging activity effects of selenium complexes **I-V** against DPPH.

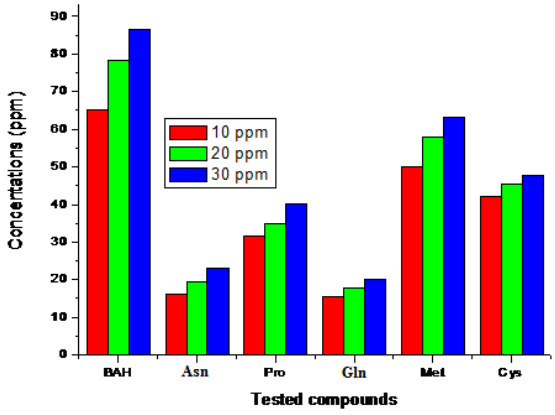

Fig. 15. Diagrams of radical scavenging activity effects of selenium complexes **I-V** against hydroxyl radicals

The Se-*Met* and Se-*Cys* displayed the highest radical scavenging activity effects against DPPH compared with BHA. In the DPPH free radical scavenging test the stable yellow-colored diphenylpicrylhydrazine (DPPH-H) is formed in the presence of an antioxidant. The scavenging effects of BHA at concentrations 10, 20 and 30 ppm on the hydroxyl radical were 65.2, 78.3 and 86.5%, respectively. When the tested compounds or BHA were incubated with the reaction mixture they were able to interfere with free radical reaction and could prevent damage to the sugar.

CONCLUSION

Selenium(IV)-amino acids complexes of *Asn*, *Pro*, *Gln*, *Met*, and *Cys* were synthesized and characterized using analytical techniques such as elemental analysis, thermal analyses and (FT–IR, Raman laser, ^{1}H-NMR, and UV–Vis) spectroscopy. The microanalytical elemental data deduced a 1:2 selenium ions: amino acid ratio of the synthesized complexes. In view of the FT-IR spectroscopy results the selenium (IV) ion was coordinated to the respective amino acids as a bidentate chelate. The geometry of the selenium ions was six-coordinated with those of amino acid complexes. The selenium in nano-structured form was investigated by Raman laser spectroscopy, X-ray powder diffraction, surface morphology, scanning electron microscopy (SEM). The free radical scavenging activity of the newly synthesized selenium (IV) complexes was determined at the concentration of 10, 20 and 30 ppm using stable DPPH free radicals. All complexes displayed a significant antioxidant activity.

***Acknowledgements**: This work was funded by the Deanship of Scientific Research at Princess Nourah bint Abdulrahman University, through the Research Groups Program Grant no. (RGP-1438-0003).*

***Author Contributions:** Ahmed Naglah, R.F. Hassan and Moamen Refat designed and observed the proposal, contributed to data analysis and interpretation. Wael Hozzien did the biological study and wrote the biological part. Asma S. Al-Wasidi, Nawal M. Al-Jafshar and Jamelah S. Al-Otifi, surveyed data in the database and did the spectral analysis. Ahmed Naglah and Moamen Refat gave conceptual advice and wrote the paper. All authors discussed the results and implications and commented on the manuscript at all stages.*

***Conflict of Interests:** The authors declare no conflict of interests.*

REFERENCES

1. Q. Wang, A. R. Parrish, L. Wang. Expanding the genetic code for biological studies, *Chem. Biol*. **16** (3), 323 (2009).
2. P. Newsholme, L. Stenson, M. Sulvucci, R. Sumayao, M. Krause. Amino Acid Metabolism. Comprehensive Biotechnology (2nd ed.), **1**, 3 (2011).
3. K. Asemave, S. G. Yiase, S. O. Adejo, B. A. Anhwange, *International Journal of Inorganic and Bioinorganic Chemistry*, **2** (1), 11 (2011).
4. R. H. Garret, C. M. Grisham, Biochemistry, Sanders, New York, 1995, p. 216.

5. J. H. Ottawa, D. K. Apps, Biochemistry, ELBS, London, 1984.
6. N. Visfiliumurthy, P. Lingaiah, *Ind. J. Chem.* (A), **25,** 875 (1986).
7. T. R. Rap, M. Sahay, R. C. Aggarwal, *St. J. Chem. (A),* **23**, 214 (1984).
8. A. Marcu, A. Stanilaa, O. Cozar, L. David; *Journal of Optoelectronics and Advanced Materials*, **10**(4), 830 (2008).
9. L. R. Dinelli, T. M. Bezerra, J. J. Sene, *Curr. Res. Chem*., **2**, 18 (2010).
10. S. S. Dara, A Textbook of Environmental Chemistry and Pollution Control, S. Chand and Company Ltd, India, 2005, p. 67.
11. B. H. Xu, K.Y. Huang, Chemistry, Biochemistry of Selenium and its Application in Life Science, Hua East University of Science & Technology Press (Ch). 1994.
12. X. Y. Gao, J. S. Zhang, L. D. Zhang, M. X. Zhu, *China Public Health,* **16**, 421 (2000).
13. B. Gates, B. Mayers, B. Cattle, Y. N. Xia, *Adv. Funct. Mater.,* **12**, 219 (2002).
14. V. V. Kopeikin, S.V. Valueva, A. I. Kipper, L. N. Borovikova, A. P. Filippov, *Polymer Science*, Series A, **45** (4), 374 (2003).
15. X. Y. Gao, J. S. Zhang, L. D. Zhang, *Adv. Mater*., **14**, 290 (2002).
16. X. Zhang, Y. Xie, F. Xu, X. H. Liu, Chin. *J. Inorg. Chem*., **19**, 77 (2003).
17. B. Gates, B. Mayers, A. Grossman, Y. N. Xia, *Adv. Mater*., **14**, 1749 (2002).
18. E. R. dos Santos, R. S. Corrêa, L. V. Pozzi, A. E. Graminha, H. S. Selistre-de-Araújo, F. R. Pavan, A. A. Batista, *Inorg. Chim. Acta*, **463**, 1, (2017).
19. M. Taha, I. Khan, J. A. P. Coutinho, *Journal of Inorganic Biochemistry*, **157**, 25 (2016).
20. S. Choksakulporn, A. Punkvang, Y. Sritana-anant, *Journal of Molecular Structure*, **1082**, 97 (2015).
21. S. Ghasemi, A. H. Khoshgoftarmanesh, M. Afyuni, H. Hadadzadeh, R. Schulin, *Soil Biology and Biochemistry*, **63**, 73 (2013).
22. P. Ramakrishnan, S. Shanmugam*, Journal of Power Sources*, **316**, 60 (2016).
23. W. Brand-Williams, M. E. Cuvelier, C. Berset, Use of a free radical method to evaluate antioxidant activity, *LWT Food Sci. Technol*., **28**, 25 (1995).
24. H. Ohkawa, N. Ohishi, K. Yagi, Assay for lipid peroxides in animal tissues by thiobarbituric acid reaction, *Anal. Biochem*., **95**, 351 (1979).
25. K. Shimoda, K. Fujikawa, K. Yahara, T. Nakamura, Antioxidative properties of xanthan on the autoxidation of soybean oil in cyclodextrin emulsion, *J. Agric. Food Chem*., **40**, 945 (1992).
26. W. J. Geary, *Coord. Chem. Rev*., **7,** 81 (1971).
27. M. S. Refat, *J. Mol. Struct*., **842** (1–3), 24 (2007).
28. C. H. Ramamurthy, K. S. Sampath, P. Arunkumar, M. S. Kumar, V. Sujatha, K. Premkumar, C. Thirunavukkarasu, *Bioprocess and Biosystems Engineering*, **36,** 1131 (2013).
29. E.J. Baran, I. Viera, M.H. Torre, *Spectrochim. Acta,* **66A,** 114 (2007).
30. T.J. Lane, J.A. Durkin, R.J. Hooper, *Spectrochim. Acta,* **20,** 1013 (1964).
31. J.F. Jackovitz, J.L.Walter, *Spectrochim. Acta,* **22,** 1393 (1966).
32. B. Smith, Infrared Spectral Interpretation, CRC Press, Boca Raton, 1999.
33. K. Nakamoto, Infrared and Raman Spectra of Inorganic and Coordination Compounds: Part B, 5th ed., Wiley, New York, 1997.
34. G.B. Deacon, R.J. Phillips, *Coord. Chem. Rev*., **33**, 227(1980).
35. M.S. Refat and Kh. M. Elsabawy, *Bulletin of Material Sciences*, **34**(4), 873 (2011).
36. B.D. Cullity, Elements of X-ray Diffraction, Addison-Wesley Publication Company, Massachusetts, 1978.
37. M. P Rayman, The importance of selenium to human health, *The Lancet,* **356,** 233 (2000).

СИНТЕЗ, ОХАРАКТЕРИЗИРАНЕ И АНТИОКСИДАНТНА АКТИВНОСТ НА КОМПЛЕКСИ НА СЕЛЕН (IV) С НЯКОИ АМИНОКИСЕЛИНИ – БИНУКЛЕАРНИ КОМПЛЕКСИ

А. М. Наглах[1,2*], А. С. Ал-Васиди[3], Н. М. Ал-Джафшар[3], Дж. С. Ал-Отифи[3], М. С. Рефат[4, 5], У. Н. Хоцеин[6, 7]

[1] *Департамент по фармацевтична химия, Катедра по разработване и изследване на лекарства, Колеж по фармация, Университет „Крал Сауд“, Рияд 11451, Саудитска Арабия*

[2] *Департамент по химия на пептидите, Отдел по изследване на химическата индустрия, Национален изследователски център, 12622 Доки, Кайро, Египет*

[3] *Департамент по химия, Научен колеж, Университет „Принцеса Нура Бинт Абдулрахман“, Рияд 11671, Саудитска Арабия*

[4] *Департамент по химия, Научен факултет, Таифски университет, п.к. 888, Ал-Хауиа, Таиф 21974, Саудитска Арабия*

[5] *Департамент по химия, Научен факултет, Университет на Порт Саид, Порт Саид, Египет*

[6] *Катедра по изследване на биопродукти, Департамент по зоология, Научен колеж, Университет „Крал Сауд“, Рияд 11451, Саудитска Арабия*

[7] *Департамент по ботаника и микробиология, Научен факултет, Университет на Бени-Суеф, Бени Суеф 62111, Египет*

Постъпила на 9 януари, 2018 г.; приета на 17 май, 2018 г.

(Резюме)

Получени са комплексите на селен (IV) с аминокиселините аспарагин (*Asn*), пролин (*Pro*), глутамин (*Gln*), метионин (*Met*) и цистеин (*Cys*) и са охарактеризирани чрез елементен анализ, измерване на молната проводимост, спектрални изследвания (IR, Раман, UV-Vis, ^{1}H-NMR и мас-) и термогравиметричен анализ (TG/DTG). Изследванията на рентгеновата дифракция са проведени на дифрактометър PANalytical, повърхностната хомогенност на пробите е изследвана със сканиращ електронен микроскоп Quanta FEG 250 (SEM), а химичният състав на пробите е определен чрез енергийно-дисперсивен рентгенов анализ. Всички комплекси на селен (IV) **(I-V)** са от вида $[Se^{+4}(AA^{-1})_2Cl_2]$, където AA = (*Asn*, *Pro*, *Gln*, *Met* и *Cys*) се отнасят като монобазични лиганди. Масовите фрагменти на комплекса [Se $(Cys)_2(Cl)_2$] (**V**) подкрепят твърдението за монобазичност. Предполагаемата геометрия на 1:2 комплексите е октаедрична конфигурация с два хлорни атома и два бидентатни лиганда, заемащи ъгловите места в октаедричните комплекси. В комплексите на селен с *Asn*, *Pro*, *Gln* и *Met*, амино и карбоксилните групи участват в координирането с метала, докато *Cys* се координира посредством сулфхидрилната и карбоксилната група. Активността на новосинтезираните комплекси на селен (IV) за отстраняване на свободни радикали е определена при концентрация от 10, 20 и 30 ppm въз основа на взаимодействието със стабилния свободен радикал 1,1-дифенил-2-пикрилхидразил (DPPH). Всички комплекси проявяват добра антиоксидантна активност.